

Whistler Instability in an Electron-Magnetohydrodynamic Spheromak

R. L. Stenzel,* J. M. Urrutia, and K. D. Strohmaier

Department of Physics and Astronomy, University of California, Los Angeles, California 90095-1547, USA
(Received 14 June 2007; published 28 December 2007)

A three-dimensional magnetic vortex, propagating in the whistler mode, has been produced in a laboratory plasma. Its magnetic energy is converted into electron kinetic energy. Non-Maxwellian electron distributions are formed which give rise to kinetic whistler instabilities. The propagating vortex radiates whistler modes along the ambient magnetic field. A new instability mechanism is proposed.

DOI: 10.1103/PhysRevLett.99.265005

PACS numbers: 52.35.Hr, 52.35.Mw, 52.55.Ip

Whistler waves play an important role in space and laboratory plasmas [1]. They can scatter electrons in velocity space [2], thereby creating possible loss of particle confinement in mirror fields. Vice versa, whistlers can be excited by wave-particle interactions, e.g., via the Landau resonance with electron beams [3] or via the cyclotron resonance in plasmas with electron temperature anisotropies [4] such as exist in loss-cone distributions [5]. Even isotropic distributions with energetic tails (κ -Maxwellians) can significantly change the dispersion and damping of whistlers [6]. While many observations of whistler emissions and instabilities have been reported for space plasmas, far fewer reports exist for laboratory plasmas. The latter include beam-whistler [7] and loss-cone instabilities [8]. But to our knowledge, it has never been observed that the free energy for such instabilities can arise from the damping of whistler modes themselves, as is the case in the present experiment. Here we excite an unusually large whistler mode with wave magnetic field exceeding the ambient field [9]. When the topology of this wave contains a magnetic null line, it energizes the electrons more efficiently than through collisional damping. Such a nonlinear wave can be called a traveling 3D magnetic vortex or whistler spheromak whose properties have been described recently [9,10]. In the present Letter we report that the energized electrons create a new whistler instability. Small amplitude higher frequency whistlers are continuously emitted from a traveling and decaying spheromak. A physical mechanism for an absolute instability in a propagating current ring is proposed.

The experiments are performed in a large, pulsed dc discharge plasma generated with parameters as shown schematically in Fig. 1. An insulated magnetic loop antenna (4 turns, 10–15 cm diam) is inserted into the plasma center with its axis aligned along \mathbf{B}_0 and energized by a damped oscillatory current ($I_{\max} \approx 300$ A, frequency $\omega/2\pi \approx 200$ kHz $\ll \omega_c/2\pi \approx 20$ MHz). The magnetic field inside the plasma is measured with a single magnetic probe containing three orthogonal small loops (5 mm diam) which can be moved along three coordinates. The space-time dependence of the field $\mathbf{B}(\mathbf{r}, t)$ is obtained from repeated, highly reproducible discharges. The experiments are done in the quiescent afterglow plasma. A Langmuir

probe (3 mm²), attached near the magnetic probe, measures the plasma parameters in space and time.

A field-reversed configuration (FRC) is produced in the first half cycle of the antenna current and partially penetrates into the plasma. In the second half of the cycle, the antenna field adds to \mathbf{B}_0 and produces a strong single mirror field. At the first zero crossing of the antenna current, the FRC is still frozen into the plasma while the antenna begins to impose a mirror configuration. This splits it into two FRCs, and the emerging mirror field forces them apart, propagating away from the antenna via the whistler mode, self-consistently developing a toroidal field. A snapshot of the total measured field lines is shown in Fig. 2(a). The field topology is similar to that of MHD spheromaks, but a whistler spheromak is only frozen into the electron fluid and propagates without changing the ion density. Since $n_e \approx n_i$, the electrons are incompressible and their flows are rotational.

Strong electron heating is observed in the toroidal current layer of the whistler spheromak. Langmuir probe traces, such as shown in Fig. 2(b), not only demonstrate bulk electron heating (from 2 eV to 18 eV), but also formation of energetic tails (22 eV). Electron energization is indirectly confirmed by visible light emission from the spheromak in the surrounding dark afterglow plasma. Electron acceleration does not occur in the second half

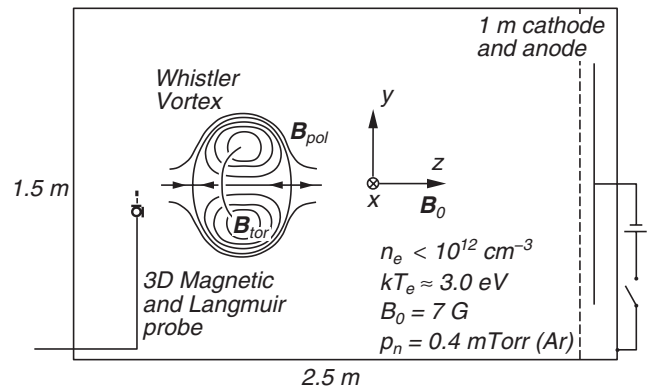


FIG. 1. Schematic of the experimental setup with typical parameters.

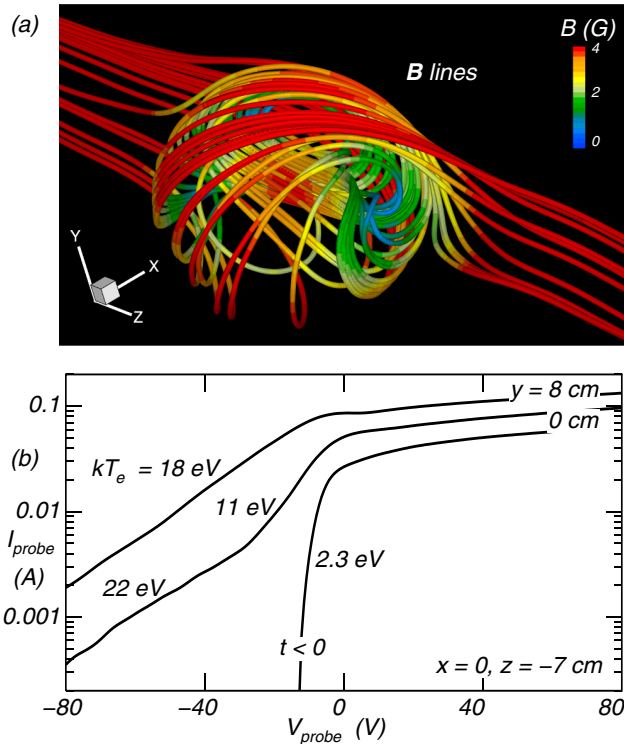


FIG. 2 (color online). (a) Measured magnetic field lines of a whistler spheromak. The spheromak has propagated 23 cm from the antenna along $-\mathbf{B}_0$. (b) Langmuir probe trace showing how the unperturbed background plasma ($t < 0$) is energized by a whistler spheromak. Energetic tails indicate non-Maxwellian distributions (center of antenna is at $x = y = z = 0$).

cycle of the antenna current when whistler modes with mirror field topology are excited. Such field topologies have no toroidal null lines and are produced by electron Hall currents which do not dissipate magnetic energy. However, the electrons can be strongly energized in a toroidal null layer and its vicinity by a toroidal electric field. Anisotropic distributions are likely to arise which could be resolved with a directional velocity analyzer and may be attempted in future work [11].

Evidence for a whistler instability is presented in Fig. 3. The expulsion of the FRCs from the antenna due to the change in sign of its current leads to local electron heating. The heat produces a whistler instability as seen in the high frequency fluctuations of the magnetic probe signal shown. No heating or fluctuations are observed during the second zero crossing of the current since it produces no toroidal null line. Whistler spheromaks are not produced below a threshold in the decaying current. The oscillations are shown on an expanded time scale at the bottom of the figure. The frequency of the dominant oscillation (7 MHz) is smaller than the electron cyclotron frequency, $f_c = eB_0/2\pi m_e \approx 20$ MHz, but much higher than the applied frequency (0.2 MHz). The unstable waves are linear waves ($B_{\text{wave}} \ll B_0$), whereas the whistler spheromak is a highly nonlinear wave phenomenon. In addition to the dominant

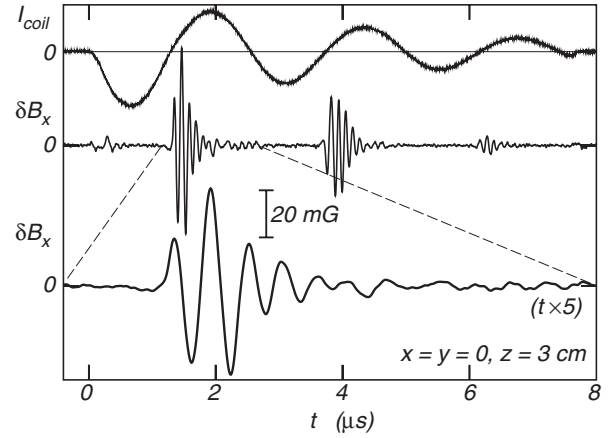


FIG. 3. Top: antenna current vs time. Middle: magnetic oscillations created during strong electron acceleration by whistler spheromaks, launched when $I \approx 0$ and $dI/dt > 0$. Bottom: oscillations on a time scale expanded by a factor 5, showing the dominant oscillation has a frequency $f \approx 7$ MHz.

oscillation, lower level emissions are also observed over a wide range of frequencies in the whistler branch.

In order to determine the instability mechanism we first investigate the properties of the unstable waves in space and time. The topology of the wave fields is shown in Fig. 4(a) which displays in the y - z plane ($x = 0$) a snapshot of a vector field of the components (B_y, B_z) superimposed on contours of B_x . The 10 cm diam antenna and spheromak are located at $z = 0$, and the 7 MHz waves shown are propagating ahead of the spheromak in the essentially uniform plasma with $B_0 = 7$ G. The observed wave pattern translates in time along \mathbf{B}_0 with little change, implying a predominantly parallel group velocity. Since the wave packets have conical phase fronts they have a range of oblique wave numbers. Only on axis where the field strength peaks is the wave topology close to that of a parallel-propagating whistler with wavelength $\lambda \approx 14$ cm.

The wave magnetic field lines in 3D space are not easy to visualize or display. For simplicity, we have decomposed them into fields lines ($\delta B_y, \delta B_z$) which approximately follow the phase fronts indicated by $\delta B_x = \text{const}$. These field lines link with similar shape, but 90° out of phase, ($\delta B_x, \delta B_z$) field lines in the x - z plane (not shown). Note that away from the spheromak the peaks in δB_x fall into the minima of δB_y and vice versa. For a wave propagating along \mathbf{B}_0 , the linkage is right handed; thus, its magnetic field helicity density is positive but reverses for the opposite propagation direction.

The topology of the unstable wave magnetic field is distinctly different from that of waves excited by the antenna. In the latter case, the wave fields have a vortex topology [12] which has a longitudinal field δB_z on axis rather than a transverse field, δB_x . Thus, the unstable waves are not excited by toroidal antenna currents δJ_θ , but by transverse currents δJ_y in the plasma.

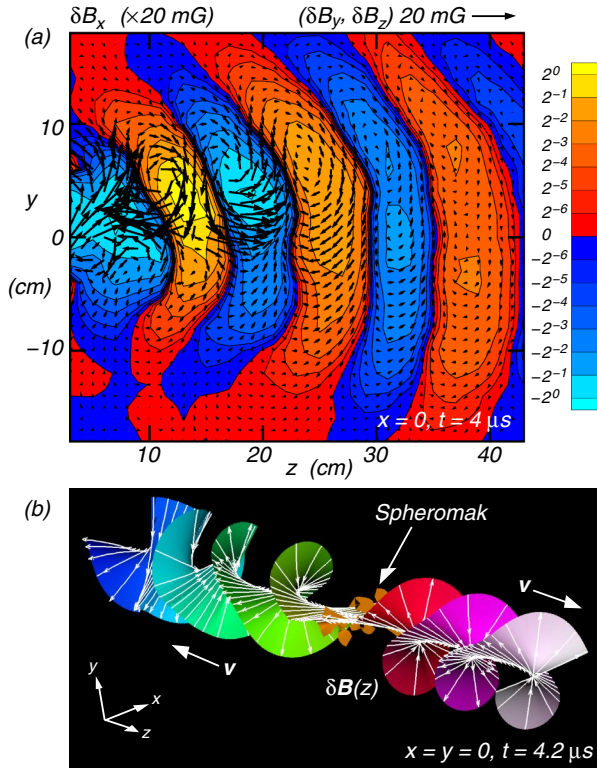


FIG. 4 (color online). Field topology and polarization. (a) Magnetic field components in the y - z plane when the ejected spheromak is near the antenna. Contours of δB_x showing the wave phase fronts. Vector field, $(\delta B_y, \delta B_z)$, showing loops linked with δB_x . (b) Hodogramlike display of the magnetic vector on axis when the spheromak has propagated to center of display. The waves are right-hand circularly polarized whistlers and propagate axially away from the slower moving spheromak.

The polarization of the wave is explained in Fig. 4(b). At different positions along the z axis ($x = y = 0$), a short portion of the local wave magnetic field line is traced in 3D space forming a display similar to a hodogram of unit vectors. In addition, a ribbon surface tangential to the field lines is created. The first few wavelengths ahead of the spheromak exhibit a clockwise rotation along z or a counterclockwise rotation in time when an observer faces the approaching wave. The field rotates in time in the same direction as electrons around \mathbf{B}_0 . These are the properties of right-hand circularly polarized whistler waves. On the left side of the spheromak, the polarization is also circular but with opposite sense of rotation in space, i.e., clockwise or right handed in space. An observer at a fixed z position looking along $+z$ or \mathbf{B}_0 will again see a clockwise vector rotation in time if the wave propagates in $-z$ direction. Thus the wave vector rotates again in the same direction as the electrons; hence, the wave is also a whistler. The time for the hodogram is chosen such that the spheromak center is located at the middle of the wave train. In the source region (spheromak), the polarization is linear which could be the result of interference between two oppositely prop-

agating waves with different polarizations in space. The wave interference also produces a standing wave pattern (nodes and extrema). Note that the reversal of propagation direction changes the sign of both the helicity of the polarization ellipse as well as the magnetic helicity density, $\mathbf{A} \cdot \mathbf{B}$.

The propagation of the whistler spheromak and the unstable whistler waves are demonstrated in a time-of-flight diagram of Fig. 5. The location of the spheromak is best displayed by contours of the toroidal current ring which creates the reversed poloidal (axial) magnetic field. The contour plot of $J_x(x = 0, y = 3 \text{ cm}, z, t)$ in Fig. 5(a) shows that the peak current propagates at $v_z \approx 60 \text{ cm}/\mu\text{s}$. Figure 5(b) shows a contour plot of the wave magnetic field $B_y(x = 0, y = 3 \text{ cm}, z, t)$. The unstable waves propagate at a higher velocity, $v_z \approx 100 \text{ cm}/\mu\text{s}$. The first waves excited therefore leave the spheromak behind and propagate into the uniformly magnetized plasma. In the wake of the spheromak wave propagation in the $-z$ direction is observed (negative slope of isocontours). Standing waves are observed in the region of the spheromak. The source for the waves cannot be the antenna since waves propagate toward it. Furthermore, test waves excited by the antenna have a different topology [12] from the present unstable waves. Thus, the source for the waves must be within the propagating spheromak which has been shown to locally energize the electrons [10].

To determine the type of instability (convective versus absolute), we have investigated whether and how a test

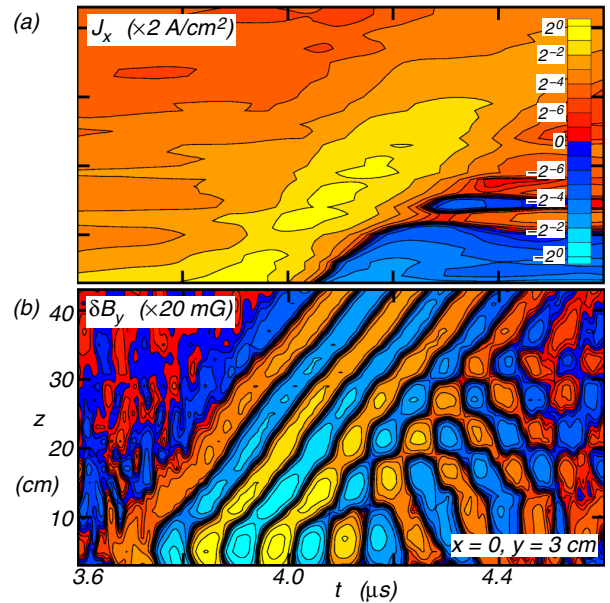


FIG. 5 (color online). Time-of-flight diagrams for (a) the spheromak and (b) the unstable whistler waves, $\delta B_y(0, 3 \text{ cm}, z, t)$. Color bar applies to both. The spheromak center is defined as the peak of the toroidal current density δJ_x . The unstable waves propagate faster than the spheromak. Note that waves travel ahead of the spheromak and are also emitted in the reverse direction (negative slope).

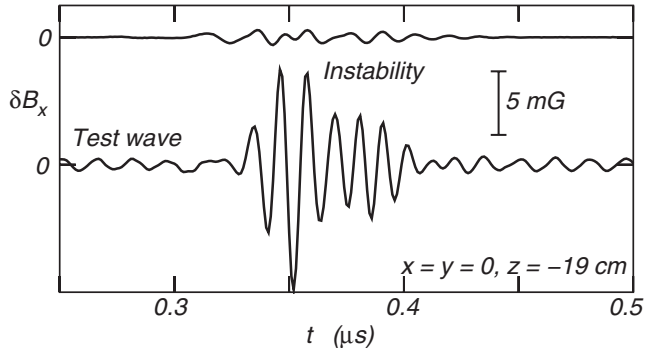


FIG. 6. Test wave experiment. Top trace: instability without test wave. Bottom trace, same vertical scale: enhanced instability amplitude in the presence of a small amplitude test wave at the instability frequency. Note that the unstable wave is up-shifted in frequency from the test wave, and, hence, is a triggered emission rather than an amplified test wave.

wave is amplified by the instability. The wave amplitudes δB_x are displayed in Fig. 6 versus time t' (arb. origin). The top trace shows the instability due to a much weaker spheromak than in previous figures created by a 15 cm diam antenna. In the bottom trace, a small amplitude whistler wave of frequency close to the instability frequency ($f \approx 7$ MHz) has been launched from an adjacent ($\Delta z = 10$ cm) 10 cm diam loop antenna. Prior to spheromak creation ($t' \leq 3 \mu s$), the test wave propagation is well understood. However, in the presence of both weak spheromak and test wave, the unstable whistler wave amplitude is enhanced by an order of magnitude. Furthermore, the amplified wave has a slightly higher frequency (9 MHz) than the test wave, different topology, and partly propagates toward the exciter antenna (not shown). Thus, the test wave is not amplified but triggers an enhanced emission from the spheromak.

The observed whistler instability is likely to arise from anisotropies in the electron distribution function. However, it is not a convective instability since the source region (spheromak) has an axial extent of order of the unstable wavelength $\lambda_{\parallel} \approx 15$ cm. It would require a growth rate on the order of the frequency for significant axial wave growth through the spheromak. Such large growth rates cannot be explained by whistler instabilities in high-beta plasmas. A more likely scenario is that the instability grows in the toroidal direction where the current density and heating are the highest and the circular geometry provides feedback for an absolute instability. Electrons in the toroidal null line are freely accelerated by the inductive electric field associated with the decaying poloidal magnetic field. Anisotropies can arise adjacent to the null layer where nonadiabatic electrons are accelerated across weak fields. If toroidal $m = \pm 1$ eigenmodes were excited, their frequency would be determined by the electron velocity and circumference of the current ring, yielding $f = v_e/2\pi r \approx 7$ MHz for $r = 5$ cm and 10 eV electrons. Excitation of toroidal eigen-

modes would be consistent with the observed linear polarization and standing waves in the source region while coupling to propagating whistler modes along $\pm \mathbf{B}_0$. The test wave experiment also excludes the possibility of a convective instability, as it triggers an enhanced emission of an absolutely unstable system. Without the test wave, the instability is triggered by the transient formation of the spheromak. In time, the natural instability loses phase coherence while the driven instability is more coherent. The fact that the test wave greatly enhances the unstable wave shows that the natural instability removes only a small fraction of the free energy in the electron distribution. We have also observed these instabilities when two counterpropagating spheromaks merge into a stationary whistler FRC. Waves are emitted from the stationary FRC region during its relaxation. Since an FRC has no poloidal currents the instability must be driven by the toroidal current ring.

In summary, we have shown that a large amplitude whistler mode with magnetic null lines modifies the electron distribution in such a way as to create a new whistler instability. Although most of the magnetic energy of the whistler spheromak is converted into electron thermal energy some of it is reconverted into wave magnetic field energy. Such processes should be of interest in Hall magnetic reconnection and strong whistler turbulence.

The authors gratefully acknowledge support from NSF-DOE and AFOSR.

*stenzel@physics.ucla.edu

<http://www.physics.ucla.edu/plasma-exp/>

- [1] R.A. Helliwell, *Whistlers and Related Ionospheric Phenomena* (Stanford University Press, Stanford, CA, 1965).
- [2] C.F. Kennel and H.E. Petschek, *J. Geophys. Res.* **71**, 1 (1966).
- [3] K. Hashimoto and H. Matsumoto, *Phys. Fluids* **19**, 1507 (1976).
- [4] S.P. Gary and H. Karimabadi, *J. Geophys. Res.* **111**, A11224 (2006).
- [5] A.K. Tripathi and K.D. Misra, *J. Atmos. Sol. Terr. Phys.* **66**, 987 (2004).
- [6] T. Cattaert, M. A. Hellberg, and R.L. Mace, *Phys. Plasmas* **14**, 082111 (2007).
- [7] R.L. Stenzel, *J. Geophys. Res.* **82**, 4805 (1977).
- [8] R.C. Garner, M.E. Mael, S.A. Hokin, R.S. Post, and D.L. Smatlak, *Phys. Rev. Lett.* **59**, 1821 (1987).
- [9] R.L. Stenzel, J.M. Urrutia, and K.D. Strohmaier, *Phys. Rev. Lett.* **96**, 095004 (2006).
- [10] R.L. Stenzel, J.M. Urrutia, and K.D. Strohmaier, *Plasma Phys. Controlled Fusion* **49**, A17 (2007).
- [11] R.L. Stenzel, W. Gekelman, N. Wild, J.M. Urrutia, and D. Whelan, *Rev. Sci. Instrum.* **54**, 1302 (1983).
- [12] J.M. Urrutia, R.L. Stenzel, and M.C. Grisley, *Phys. Plasmas* **7**, 519 (2000).